Nontidal oceanic excitation of nutation and diurnal/semidiurnal polar motion revisited

Aleksander Brzeziński
Space Research Centre, Polish Academy of Sciences, Warsaw, Poland

Rui M. Ponte
Atmospheric and Environmental Research, Inc., Lexington, Massachusetts, USA

Ahmed H. Ali
Raytheon ITSS, Pasadena, California, USA

Received 27 February 2004; revised 22 July 2004; accepted 7 September 2004; published 24 November 2004.

[1] A new 7.5-yearlong time series of hourly estimates of nontidal ocean angular momentum, representing signals forced by 6-hourly surface atmospheric pressure and winds including those forced by the atmospheric tides, is used to assess the influence of a dynamic ocean on nutation and on diurnal and semidiurnal polar motions. Using available atmospheric angular momentum data, we estimate the total excitation by the dynamically coupled atmosphere-ocean system and compare it to that of the atmosphere alone. In case of the retrograde diurnal excitation, significant contributions are found for the retrograde annual, prograde annual, and prograde semiannual nutations and for the constant offset of the celestial pole. For the prograde annual nutation corresponding to the retrograde S_1 component of excitation, the atmosphere-ocean model does not improve the agreement with VLBI observations beyond that obtained using the atmosphere model alone. We also considered separately an irregular contribution to nutation, which can excite both the free core nutation signal and other broadband variability. The irregular component of the atmosphere-ocean model is found to be significantly correlated with that derived from the atmosphere model. For the prograde diurnal component of excitation, which contributes to polar motion, the only nonnegligible effect ($\sim$9 microarc seconds (μas)) is associated with the prograde S_1 harmonic. The only significant component of the semidiurnal excitation found is the elliptical oscillation S_2 in polar motion with major semiaxis of 9 μas, but this estimate is uncertain because the 6-hourly atmospheric fields used to force the ocean do not properly resolve semidiurnal signals. In any case, this contribution is much smaller than that from the S_2 ocean gravitational tide. *INDEX TERMS:* 1210 Geodesy and Gravity: Diurnal and subdiurnal rotational variations; 1223 Geodesy and Gravity: Ocean/Earth/atmosphere interactions (3339); 1229 Geodesy and Gravity: Reference systems; 1239 Geodesy and Gravity: Rotational variations; 1255 Geodesy and Gravity: Tides—ocean (4560); *KEYWORDS:* Earth rotation, nutation, polar motion, oceanic excitation

Citation: Brzeziński, A., R. M. Ponte, and A. H. Ali (2004), Nontidal oceanic excitation of nutation and diurnal/semidiurnal polar motion revisited, *J. Geophys. Res.*, *109*, B11407, doi:10.1029/2004JB003054.

1. Introduction

[2] The interaction among atmosphere, oceans and the solid mantle is one of the most important sources of change in all three components of the Earth's rotation vector on different timescales. At diurnal and subdiurnal periods, the dominant part of the atmospheric and oceanic effects on Earth rotation is due to the gravitationally forced ocean tides. This component of the excitation is well defined in the International Earth Rotation and Reference Systems Service (IERS) Conventions 2003 [*IERS*, 2003, Tables 8.2 and 8.3] and will not be considered here in detail. The remaining part comprises the atmospheric and nontidal oceanic influences driven mostly by the daily cycle in the solar heating. (In this paper, by nontidal signals we mean any variability in the ocean that is not directly related to gravitational forcing. So-called radiational ocean tides, forced by corresponding atmospheric tides, are considered part of nontidal signals here. As the harmonic components of nontidal signals are coherent with the gravitational tides, they are usually labeled in the same way. Hence the principal diurnal and semidiurnal thermal tides are designated as S_1 and S_2, and their side lobes generated by the annual and semiannual modulations as ψ_1, K_1, P_1, P_2, T_2, R_2, etc., [see, e.g., *Dehant et al.*, 1996; *Bizouard et al.*, 1998; *Brzeziński et al.*, 2002].

0148-0227/04/2004JB003054$09.00

The same convention is followed here.) Nontidal effects in Earth rotation are only of the order of 0.1 milliarc second (mas) but nevertheless already well detectable by space geodesy techniques and very interesting from the point of view of the underlying physical processes. Their estimation is rather difficult because it requires the capability to model the circulation of the atmosphere and oceans on a global scale at subdiurnal resolution.

[3] Back in 1992, several meteorological centers started to estimate the atmospheric angular momentum (AAM) functions at 6-hour intervals [*Salstein et al.*, 1993]. *Brzeziński* [1994b] used available series to study the diurnal and semidiurnal signals in the equatorial AAM components and to estimate the corresponding effect on nutation and polar motion. Following his concept, *Bizouard et al.* [1998] estimated the atmospheric contribution to nutation using a 19-yearlong series from the U.S. National Centers for Environmental Prediction, National Center for Atmospheric Research (NCEP-NCAR) reanalysis [*Kalnay et al.*, 1996]. The most important contributions to the nutation amplitudes were found to be the prograde (counterclockwise) annual at 77 microarc seconds (μas), retrograde (clockwise) annual (53 μas) and prograde semiannual (45 μas), and to the constant offset of the celestial pole ($\delta\psi\sin\varepsilon_o = -86$ μas, $\delta\varepsilon = 77$ μas, where $\delta\psi$, $\delta\varepsilon$ are the corresponding increments in longitude and obliquity, and ε_o is the mean obliquity at the standard reference epoch t_o = J2000). In addition they discovered that the atmospheric contributions to the nutation amplitudes exhibit time variability at the level of 0.1 mas. An important observation was that these estimates agreed reasonably well with the very long baseline interferometry (VLBI) observations of nutation.

[4] *Petrov* [1998] also estimated the atmospheric contributions to the prograde diurnal and to the semidiurnal components of polar motion; see also *Brzeziński et al.* [2002] for summary of his results. In the first case the largest amplitude was for the S_1^+ term, about 7 μas. (Note that the S_1 signal in the equatorial component of the atmospheric and oceanic excitation has two distinct harmonic components, the retrograde one migrating with the Sun from east to west, and the prograde one which has the same period but the opposite direction. The retrograde component contributing to the prograde annual nutation is denoted as S_1^- while the prograde component contributing to prograde diurnal polar motion is denoted as S_1^+. The superscripts are just the signs of the corresponding frequencies. This labeling convention will also be applied to other tidal lines discussed in the paper.) In the second case, the 6-hourly sampling of the AAM series did not allow discerning between prograde and retrograde semidiurnal terms; assuming an equal size for both contributions led to an amplitude around 3 μas.

[5] *Bizouard et al.* [1998] used two available versions of the AAM pressure term, one with the so-called inverted barometer (IB) correction representing a static response of the ocean to atmospheric pressure forcing, and one without any such correction hereafter referred to as non-IB model. They found considerably better agreement with the VLBI nutation data in case of the non-IB assumption, confirming earlier claims that the IB correction is a good approximation at seasonal timescales but not adequate at periods of the order of 1 day [see, e.g., *Eubanks*, 1993, and references therein]. *Bizouard et al.* [1998] indicated a clear need for more adequate modeling of the ocean response to the atmospheric forcing when computing the geophysical fluid effects on nutation.

[6] There were several attempts in the past to estimate the dynamic response of the ocean to the atmospheric pressure variations [e.g., *Dickman*, 1988, 1998; *Ponte*, 1993]. *Dehant et al.* [1996] estimated the atmospheric pressure perturbations on nutation using the IB and non-IB models and various kinds of figures (ellipsoid, geoid, topography) to compute the diurnal torques on the Earth. The first nontidal oceanic angular momentum (OAM) series with sufficient time resolution (6 hours) was that of *Ponte* [1997]. It was estimated from the output of a 3-yearlong run of a barotropic near-global ocean model, driven with 6-hourly atmospheric wind and pressure fields from the NCEP archives. *Petrov et al.* [1998] used this series in a first attempt to compute the nontidal oceanic contribution to nutation. The OAM series was noisier than the AAM series in the nutation band and exhibited only the S_1^- peak contributing to the prograde annual nutation. Important conclusion was that accounting for OAM signals degraded the fit to the VLBI data in comparison to the fit obtained with only atmospheric non-IB signals. The most likely reason for such discrepancy was the sensitivity of the ocean results to the poorly constrained bottom friction parameters in the model.

[7] This work is a development and extension of the study by *Petrov et al.* [1998]. We apply a similar algorithm to a new 7.5-yearlong OAM hourly series computed from a barotropic model with improved representation of dissipation processes [*Ponte and Ali*, 2002]. We extract from this OAM series the retrograde diurnal signal and estimate the corresponding contributions to the nutation amplitudes, to the precession and to the constant offset of the celestial pole. In addition, we also compute the nontidal oceanic contribution to the prograde diurnal and to the retrograde and prograde semidiurnal components of polar motion. The nontidal oceanic contributions to nutation and diurnal/semidiurnal polar motion are compared to atmospheric and other known influences, as well as to available VLBI estimates of the nutation amplitudes. Important issues addressed here include the difference between the total angular momentum of the atmosphere-ocean system in the case of a dynamic ocean response to atmospheric forcing and in the case of the IB and non-IB models, and the relevance of dynamic ocean effects for closing excitation budgets at diurnal and semidiurnal periods, as well the relative importance of nontidal versus tidal effects and the sensitivity of OAM results to ocean model assumptions.

2. Theory

[8] Variations in the direction of the rotation axis are usually classified as polar motion when they involve motion with respect to the Earth crust, and as precession-nutation when they involve motion with respect to inertial space. The precession-nutation is excited by the equatorial torques on the solid mantle, which have retrograde nearly diurnal periods, as seen from the rotating Earth, and long periods with respect to the inertial space. Large part of these torques is exerted by the Moon, the Sun, and, to a lesser extent, by

the planets (astronomical variations). The remaining part is produced by the large-scale processes leading to fluctuations in the angular momentum of the atmosphere and oceans (geophysical variations). A dominant part of the geophysical variation with nearly diurnal retrograde frequencies is due to the ocean tides while the remainder comprises the atmospheric and nontidal oceanic influences driven mostly by the diurnal cycle in the solar heating. This small part, with amplitudes between 0.1 and 0.3 mas, can be separated into a regular part comprising the contributions to the nutation amplitudes, to the precession and to the constant offset of the celestial pole, and an irregular component which is particularly important as a potential source of excitation for the free core nutation (FCN).

[9] The equatorial torques on the solid Earth within other frequency bands considered in this study, prograde diurnal and retrograde/prograde semidiurnal, excite variations in polar motion below 1 mas, which are much smaller than the astronomical nutation and long periodic polar motion. The main contribution is from the ocean tides while the atmospheric and nontidal oceanic effects are only of the order of 10 μas. In addition, there is a direct effect of the tidal gravitation which is up to 50 μas for the prograde diurnal component and below 1 μas at the semidiurnal frequencies [see *IERS*, 2003, Table 5.1].

[10] A convenient way of studying the geophysical influences on polar motion and on precession-nutation is the angular momentum approach. The equatorial excitation by any disturbing medium is expressed by the so-called effective angular momentum (EAM) function $\chi = \chi_1 + i\chi_2$, with $i = \sqrt{-1}$ defined by *Barnes et al.* [1983] and rederived using more up-to-date models and constants by *Eubanks* [1993]. When considering only the atmosphere or the ocean, we will apply the usual terminology by designating the EAM as the atmospheric angular momentum (AAM, χ^A) or the oceanic angular momentum (OAM, χ^O). The EAM function consists of the matter term χ^p, which can be estimated from the global fields of atmospheric surface pressure or ocean bottom pressure, and the motion term χ^w, which depends on the global wind fields or ocean currents.

[11] Geophysical excitation of polar motion is governed by the law of conservation of angular momentum. We will use its linear approximation, the so-called broadband Liouville equation derived by *Brzeziński* [1994a] on the basis of the dynamical theory of *Sasao and Wahr* [1981]. When expressed in the frequency domain, this equation takes the form

$$p(\sigma) = \frac{\sigma_c}{\sigma_c - \sigma}\left[\chi^p(\sigma) + \chi^w(\sigma)\right] + \frac{\sigma_c}{\sigma_f - \sigma}\left[a_p\chi^p(\sigma) + a_w\chi^w(\sigma)\right], \tag{1}$$

where $p = p_x - ip_y$ describes the change in the terrestrial direction of the axis of the celestial intermediate pole (CIP), that is polar motion, $a_p = 9.2 \times 10^{-2}$, $a_w = 5.5 \times 10^{-4}$ are dimensionless constants, σ denotes the angular frequency and

$$\sigma_c = \frac{\Omega}{T_c}\left(1 + \frac{i}{2Q_c}\right), \qquad \sigma_f = -\frac{\Omega}{T_f}\left(1 - \frac{i}{2Q_f}\right) \tag{2}$$

are the Chandler and the FCN angular frequencies of resonance with imaginary parts accounting for dissipation. In equation (2), Ω denotes the diurnal sidereal frequency, that is $\Omega = +1$ cycle per sidereal day (cpsd), T_c, T_f are the resonant periods expressed in sidereal days, and Q_c, Q_f are the corresponding quality factors. In the computation we will adopt the following values determined from the observations: $T_c = 434$, $Q_c = 175$, $T_f = 1 - 1/431$ and $Q_f = 30{,}000$. Equation (1) is expressed in a rotating body-fixed terrestrial reference system having origin at the geocenter, the z axis toward the North Pole, the x axis in the plane of the Greenwich prime meridian, and the y axis in the direction 90°E, completing the right-handed triad. Note that by convention the y component of the pole, denoted here by p_y, is counted positive toward the 90°W longitude direction opposite to that of the y axis of the terrestrial system.

[12] For long periodic polar motion ($|\sigma| \ll \Omega$) including the seasonal and the Chandler wobbles, the second term on the right-hand side of equation (1) is much smaller than the first term and is therefore usually neglected in excitation studies. Consequently, the matter and the motion terms of the EAM are usually combined as a single excitation function $\chi = \chi^p + \chi^w$. Within the retrograde diurnal frequency band ($\sigma \approx -\Omega$) corresponding to nutation, the situation is different. The second term expressing the FCN resonance becomes dominant for χ^p. In case of χ^w, the role of the second term is less obvious because the transfer coefficient a_w is about 170 times smaller than a_p and that can counterbalance the resonant enhancement by the FCN. If we assume the excitation by the matter term only, that is $\chi^w = 0$, we find that the ratio $|p/\chi^p|$ changes rapidly within the nutation band. At the frequencies ψ_1^-, K_1^-, S_1^-, and P_1^-, which are the only significant spectral lines in the atmospheric and nontidal oceanic excitation of nutation (see *Dehant et al.* [1996], *Bizouard et al.* [1998], and results of section 4.1), this ratio equals 0.534, 0.092, 0.041, and 0.026, respectively. The corresponding values for the excitation by the wind term, $|p/\chi^w|$, are 0.005, 0.002, 0.002, and 0.002. The discrepancy between a_p and a_w also implies that in any excitation study concerning the nutation band χ^p and χ^w must be treated separately. Within the prograde diurnal ($\sigma \approx \Omega$), retrograde semidiurnal ($\sigma \approx -2\Omega$), and prograde semidiurnal ($\sigma \approx 2\Omega$) frequency bands, the ratio $|p/\chi|$ varies smoothly with σ, taking the approximate values of 0.002, 0.001, and 0.001, respectively, and the contribution from the second term of equation (1) is not larger than 5%, 7%, and 18% of the total excitation, respectively.

[13] Let us consider now the case of nearly diurnal retrograde perturbation of geophysical origin. This perturbation is usually expressed in terms of the incremental nutation angles in longitude $\Delta\psi$ and in obliquity $\Delta\varepsilon$ and/or as the corrections to the amplitudes of the periodical components of nutation, which have been monitored since 1979 by the VLBI technique. The celestial perturbation of the pole can be equivalently expressed with respect to the terrestrial system, that is as polar motion, by using the following relationship:

$$p = -P\, e^{-i\phi}, \tag{3}$$

where $p = p_x - ip_y$ denotes polar motion, $P = \Delta\psi \sin\varepsilon_o + i\Delta\varepsilon$ is the complex combination of the X and Y components of

the CIP in the (nonrotating) true equatorial plane, and $\phi = \Omega(t - t_o) + \phi_o$ is the Greenwich sidereal time in which ϕ_o is a quasi-constant phase; see [*Brzeziński and Capitaine*, 1993] for a proof of equation (3) and further details. In the linear approximation applied here it can be assumed that ϕ_o = const. Below, we will understand by nutation the celestial perturbation of the pole, expressed by *P*, that is comprising not only the periodical components but also the linear change related to precession, the constant offset and irregular variability.

[14] *Brzeziński* [1994a] introduced the celestial effective angular momentum (CEAM) function χ'

$$\chi = -\chi' \, e^{-i\phi} \tag{4}$$

which, from comparison of equations (3) and (4), is the EAM function χ expressed in the nonrotating celestial system. It can be shown that after substituting equations (3) and (4) into equation (1), equation (1) remains valid with *p*, χ replaced by *P*, χ' and the resonant frequencies σ_c, σ_f in the denominators replaced by their space-referred counterparts $\sigma_c' = \sigma_c + \Omega$, $\sigma_f' = \sigma_f + \Omega$; see *Brzeziński* [1994a] for a prove and further details.

[15] The transformation (4) should be followed by an appropriate smoothing in order to make χ' consistent with *P* which by convention (Resolution B1.7 of the IAU General Assembly 2000, reproduced by *IERS* [2003, Appendix]) contains only variations with periods longer than 2 days. All variations in χ with nearly diurnal retrograde frequencies ($\sigma \approx -\Omega$) become long periodic in χ'. For those diurnal tides which play important role in χ^A and χ^O, S_1^- with frequency $\sigma = -\Omega(1 - 1/366.26)$, K_1^- with $\sigma = -\Omega$, ψ_1^- with $\sigma = -\Omega(1 + 1/366.26)$, and P_1^- with $\sigma = -\Omega(1 - 2/366.26)$, the corresponding frequencies in χ' are $\sigma' = \Omega/366.26$ (prograde annual), $\sigma' = 0$ (constant), $\sigma' = -\Omega/366.26$ (retrograde annual), and $\sigma' = 2\Omega/366.26$ (prograde semiannual). Note that this transformation does not change the amplitudes of the harmonic components. All fluctuations in χ which are outside the diurnal retrograde band become short periodic in χ' (long periodic variation including seasonal effects becomes prograde diurnal, prograde diurnal–prograde semidiurnal, etc.) therefore are filtered out by the smoothing.

[16] If we apply the inverse transformation (equation (4)) to the smoothed CEAM function χ', the whole procedure becomes just a band-pass filtering of χ. However, we prefer to investigate the excitation problem in terms of χ'. One reason is that we can directly compare this transformed excitation parameter to the reported nutation parameter *P*. Another reason is that we can make a decimation of the time series of χ' in accordance with the degree of smoothing, which greatly reduces the number of data without any significant loss of information.

[17] Mathematically, the above procedure of transformation $\{p, \chi\} \rightarrow \{P, \chi'\}$ is known as the complex demodulation at frequency $\sigma_o = -\Omega$. According to *Bingham et al.* [1967, p. 58], "complex demodulation can be considered to be a method of producing the low-frequency 'images' of more or less gross frequency components of a time series." From the elementary property of the Fourier transform $\mathcal{F}[f(t)e^{-i\sigma_o t}](\sigma) = \mathcal{F}[f(t)](\sigma + \sigma_o)$ it follows that although the original functions have been changed significantly by the demodulation, their Fourier transforms have only been shifted along the frequency axis in such a way that the demodulation frequency σ_o becomes 0. Quoting again from *Bingham et al.* [1967, p. 58], "computationally, each frequency band of interest is shifted to zero and the result run through a low-pass filter." One advantage of the complex demodulation procedure is that we employ in the subsequent analyses only the slowly varying quantities which significantly reduces the amount of data in the derivations.

[18] The concept of complex demodulation can be easily extended to other high-frequency bands of excitation considered in this paper. We express the variations with frequencies from the vicinity of $n\Omega$ (prograde diurnal for $n = 1$, retrograde/prograde semidiurnal for $n = -2/+2$) by

$$p = -p_n e^{in\phi}, \qquad \chi = -\chi_n e^{in\phi}. \tag{5}$$

After applying the low-pass filtering, or smoothing, the slowly varying quantities p_n, χ_n will be called the complex demodulate of *p*, χ at frequency $n\Omega$. *Brzeziński* [2000] showed that the corresponding modification of equation (1) consists in replacing *p*, χ by p_n, χ_n and the resonant frequencies σ_c, σ_f in the denominators by $\sigma_{c,n} = \sigma_c - n\Omega$, $\sigma_{f,n} = \sigma_f - n\Omega$ which are the frequencies of the CW and FCN resonances referred to the demodulation frequency $n\Omega$.

[19] The selection of $n\Omega$ for representing the spectral bands under consideration is obvious only in case of nutation ($n = -1$) and quite natural (for the reason of symmetry with the nutation band) in case of prograde diurnal polar motion ($n = +1$). For the semidiurnal polar motion it might be justified to use the frequencies of the S_2^- and S_2^+ tides instead of -2Ω and $+2\Omega$. Such replacement would not change the estimation of the harmonic model in the semidiurnal band, considered below, and only shift the corresponding spectral plots along the horizontal axis. However, the time domain plots of the demodulated series would be changed significantly.

[20] Finally, as noted by *Brzeziński et al.* [2002], for the NCEP/NCAR reanalysis AAM series, there is aliasing between the spectral components in the retrograde and prograde semidiurnal bands; see also section 4.3. However, this is entirely due to the 6-hourly sampling of AAM which is not sufficient to resolve the semidiurnal band. More importantly, the demodulation procedure itself does not introduce aliasing or any other undesired effect. Further details concerning application of the complex demodulation for studying high-frequency excitation of Earth rotation are given by *Brzeziński* [1994a], *Bizouard et al.* [1998], *Brzeziński* [2000], and *Brzeziński et al.* [2002].

3. Excitation Series

[21] *Ponte* [1997] introduced the use of barotropic (constant density) models for the study of nontidal OAM signals and their effects on Earth rotation. Such models can be easily driven by both wind stress and atmospheric pressure and have proven to be a very useful tool in the study of rapid signals in polar motion and length of day [*Nastula and Ponte*, 1999; *Ponte and Ali*, 2002]. The oceanic excitation functions χ_1^O and χ_2^O used in the present study are based on the barotropic modeling efforts described by *Ponte and Ali*

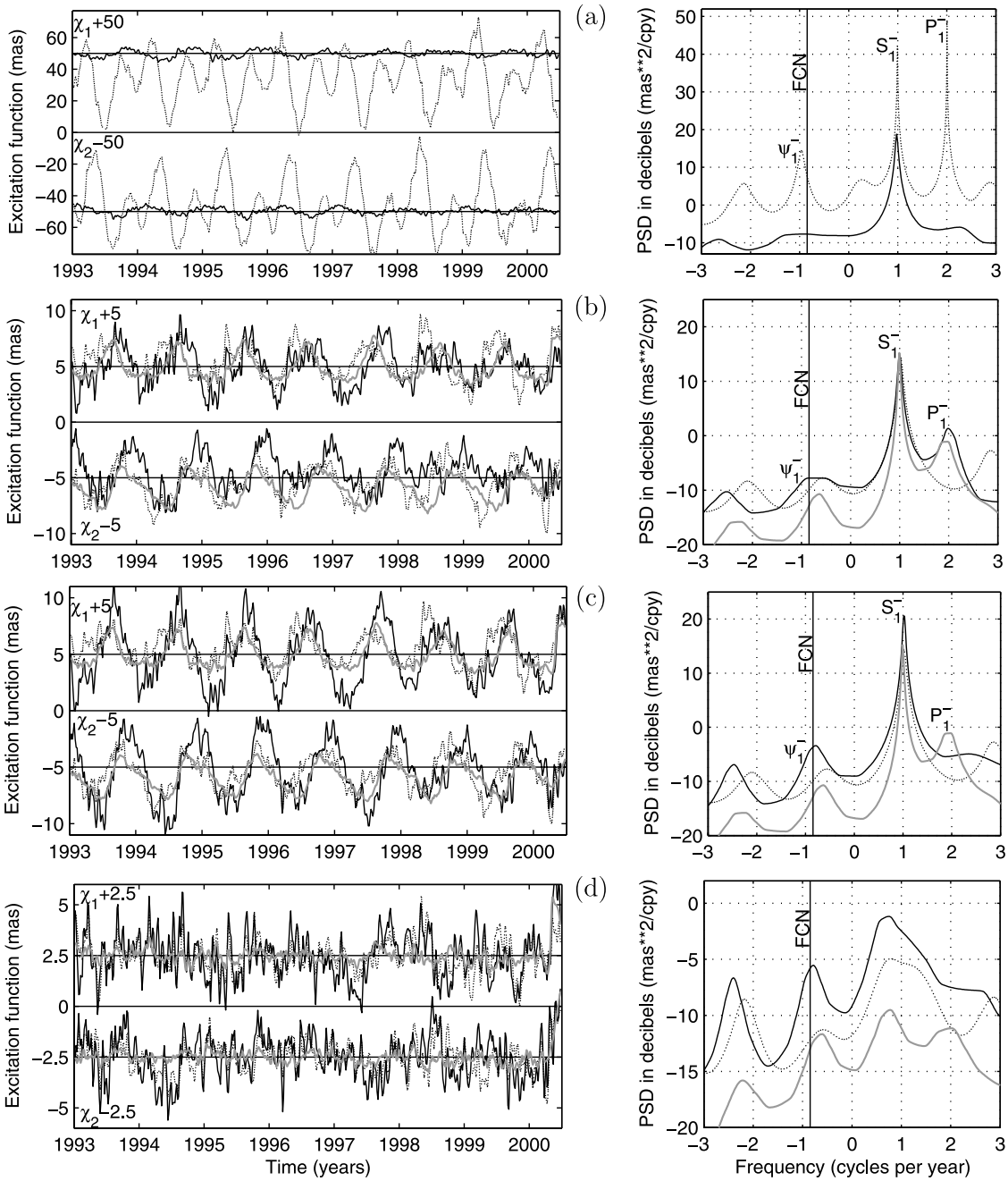

Figure 1. Celestial effective angular momentum (CEAM) functions, that is, the EAM functions demodulated at the frequency −1 cpsd, of the atmosphere and of the ocean. (left) Time domain representation of CEAM and (right) maximum entropy estimate of the corresponding power spectral density (PSD) function (note that the tidal codes used to identify the spectral peaks refer to the original EAM functions). The following terms of the excitation are shown: (a) the motion terms of AAM (blue) and OAM (black); (b) the matter terms of AAM (blue), AAMIB (red), and OAM (black); (c) the matter terms of the system atmosphere/ocean for different models of the ocean response to atmospheric forcing: AAM (blue), AAMIB (red) and AAMIB + OAM (black); see text for additional discussion; and (d) same as in Figure 1c but after removal from each signal of the model comprising the first-order polynomial and sinusoids with periods ±1, ±1/2, and ±1/3 years (see Table 1 for the parameters of the model). See color version of this figure at back of this issue.

[2002]. Details of the model and its configuration are given by *Ponte and Ali* [2002, and references therein], and thus only a few relevant issues are revisited here.

[22] The ocean model is driven by surface wind and pressure fields from the NCEP-NCAR reanalysis [*Kalnay et al.*, 1996], available at 6-hour intervals on a 2.5° by 2.5° horizontal grid. The forcing fields are linearly interpolated to the model time step (60 s) and bilinearly interpolated to the model grid (1.125° × 1.125°). From the simulated sea level and velocity fields, χ_1^O and χ_2^O values are calculated using the formulation of *Barnes et al.* [1983]. The matter terms are computed based on fluctuations in adjusted sea level, that is, sea level minus the IB correction as defined by *Ponte* [1997].

[23] Hourly values of χ_1^O and χ_2^O for the period January 1993 to June 2000 are used in the subsequent analyses. Note, however, that there is essentially no forcing at periods <12 hours, apart from signals introduced by the linear interpolation of the 6-hourly NCEP-NCAR fields. Thus simulated variability at those short periods is of little value. More importantly, the 6-hour sampling is not sufficient to resolve the full nature of the S_2 barometric tide [e.g., *Ponte and Ray*, 2002], and the linear interpolation of the 6-hour fields also affects the representation of the S_1 barometric tide. These caveats in the representation of the forcing should be kept in mind in the interpretation of our results.

[24] Atmospheric excitation functions χ_1^A and χ_2^A spanning the same period were obtained from the IERS Special Bureau for the Atmosphere [*Salstein et al.*, 1993]. For consistency with the forcing fields used to drive the ocean model, χ_1^A and χ_2^A values are calculated [*Salstein et al.*, 1993] from NCEP-NCAR reanalysis winds and surface pressure fields [*Kalnay et al.*, 1996]. As usual, so-called non-IB and IB matter terms are both considered. Non-IB series are based on the full variability of the pressure fields; IB series assume an isostatic ocean response to atmospheric pressure fluctuations and thus only include effects of variability in the average atmospheric pressure over the ocean. The IB formulation is used when combining χ^A with χ^O, consistent with the calculation of the latter in terms of adjusted sea level. The 6-hourly χ^A values present the same resolution problems for the semidiurnal variability noted for χ^O.

4. Data Analysis and Results

[25] We process all terms of the OAM and AAM series in a similar way as *Bizouard et al.* [1998] and *Petrov et al.* [1998] and by applying the methods described in detail by *Brzeziński et al.* [2002]. First, by using equations (4) and (5) we compute the complex demodulate of χ^A and χ^O at frequencies $-\Omega$, $+\Omega$, -2Ω and $+2\Omega$. Each demodulated series is then smoothed by a Gaussian filter with full width at half maximum equal to 10 days and sampled at equidistant 5-daily intervals starting from modified Julian date (MJD) 48,995.0. That reduces series to 546 points compared to 65,712 points in the original hourly OAM series. Each series is spectrally analyzed by applying the maximum entropy method (MEM) algorithm developed by *Brzeziński* [1995]. The demodulated series and the corresponding MEM power spectra are shown in Figures 1a, 1b, 1c, 2a, 2b, 2c, 3a, and 3c. Note that the frequencies of the spectral plots concern the demodulated series, while the tidal code used to label the spectral peaks refer to the original AAM and OAM series. In contrast to previous works [*Bizouard et al.*, 1998; *Petrov et al.*, 1998], the spectral plots in Figures 1–3 do not contain the zero-frequency peak because we remove the sample mean from each input time series prior to the spectral estimation.

[26] We estimate for the demodulated series AAM and OAM the best least squares fit of the model which is a sum of the complex sinusoids with periods ±1 year, ±1/2 years, and ±1/3 years and the first-order polynomial. Such a model comprises all terms which could be detected by the spectral analysis, on the other hand each component of the model has a physical explanation, either as being excited by the thermal tides S_1, S_2, or as expressing the seasonal modulation of these tides; see *Dehant et al.* [1996] and *Bizouard et al.* [1998, Appendix A] for explanation. This model is used in equation (1) to compute the corresponding influence on nutation and polar motion. Results of the estimation are shown in sections 4.1–4.3. After removing this model we compute once more the power spectrum and compare various excitation terms. Results are shown in Figures 1d, 2d, 3b, and 3d. In the following discussion we will refer to the demodulated excitation series simply as AAM or OAM. The reader should bear in mind, however, that the long periodic components (semiannual, annual, constant) in the demodulated series correspond to the quasi diurnal or quasi semidiurnal periodicities in the original series, as it was discussed in section 2 and is marked by the tidal codes in the spectral plots of Figures 1–3 and in the description of various components shown in sections 4.1–4.3.

4.1. Excitation of Nutation

[27] In case of the motion term (Figure 1a and Table 1) the oceanic contribution is small in comparison to the large prograde semiannual and annual variations and constant offset seen in the AAM wind term. This is very different from results in previous subdaily barotropic ocean model of *Ponte* [1997], for which the oceanic signals were smaller by only a factor of ∼2 [*Petrov et al.*, 1998]. As before, the OAM power spectrum exhibits only the S_1 peak superimposed on the flat background. From Table 1 the only nonnegligible excitation from ocean currents is for the prograde annual nutation (∼4.5 μas).

[28] In case of the mass term (Figure 1b), OAM is of comparable size to AAM and AAMIB and slightly delayed in time, as expected. Its power spectrum shows a structure similar to that of AAM, with the main S_1^- peak expressing the diurnal thermal (radiational) tide and its side lobes expressing the seasonal modulation of the S_1 tide. When considering the influence on nutation, more important is the comparison of the excitation functions representing the whole atmosphere-ocean system corresponding to various models of the ocean response to the atmospheric forcing: the non-IB model, which assumes a rigid ocean, with the aggregated excitation expressed just by AAM; the IB model with the excitation expressed by AAMIB series; and the dynamic model with the excitation expressed by the sum OAM + AAMIB. The matter terms of these three excitations are compared in Figure 1c. Inspection of the time domain plots shows that the dynamic model has considerably larger amplitude and is delayed in time relative to the

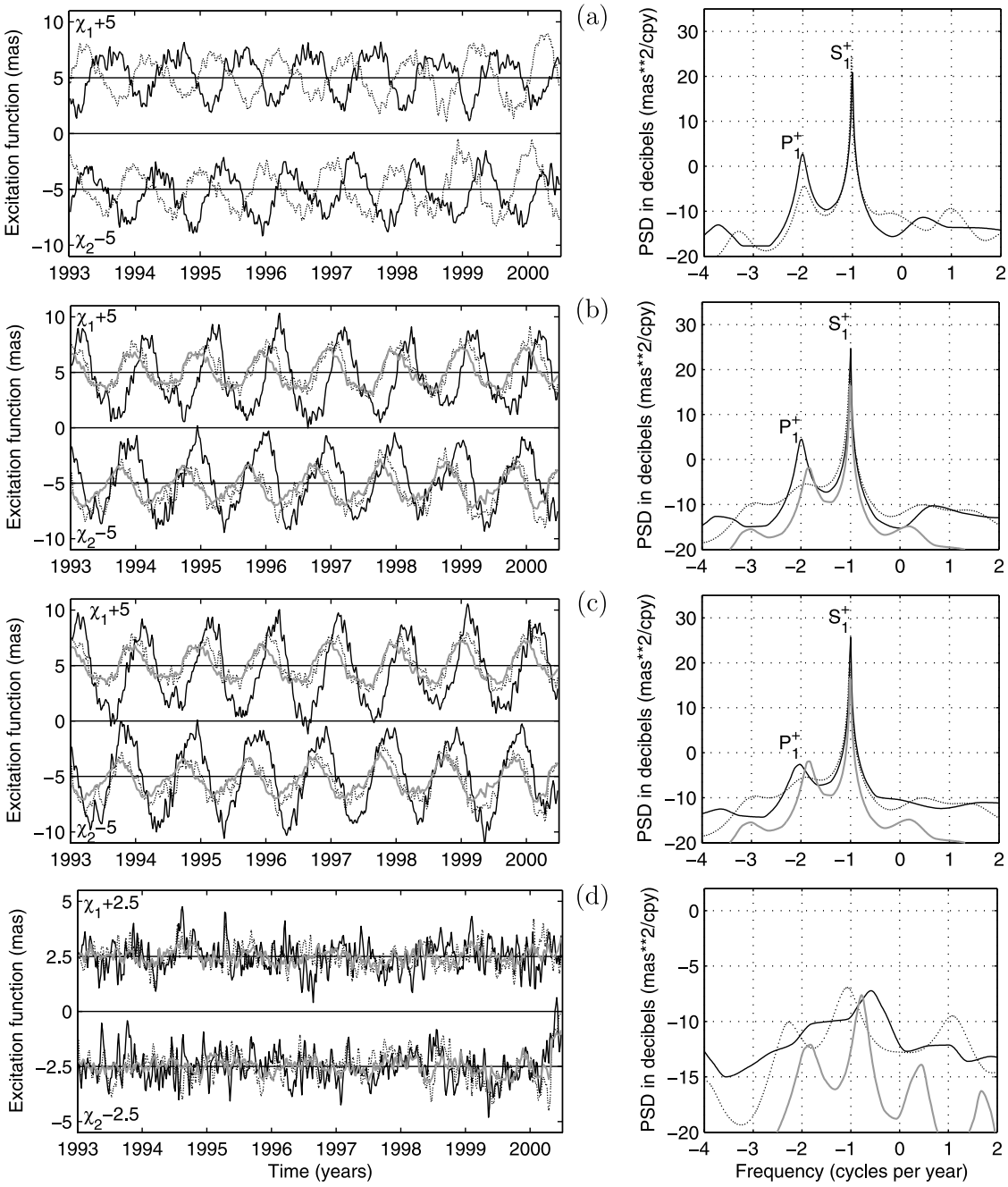

Figure 2. Effective angular momentum (EAM) functions of the atmosphere and of the ocean, demodulated at frequency +1 cpsd. (left) Time domain representation and (right) corresponding maximum entropy power spectra (note that the tidal codes used to identify the spectral peaks refer to the original EAM functions, before demodulation). The following terms of the excitation are shown: (a) the motion terms of AAM (blue) and OAM (black); (b) the matter terms of AAM (blue), AAMIB (red), and OAM (black); (c) the matter terms of the system atmosphere/ocean for different models of the ocean response to atmospheric forcing: AAM (blue), AAMIB (red) and AAMIB + OAM (black); see text for additional discussion; and (d) same as in Figure 2c but after removal from each signal of the model comprising the first-order polynomial and sinusoids with periods ±1, ±1/2, ±1/3 years (see Table 3 for the parameters of the model). See color version of this figure at back of this issue.

other two models. Comparison of the power spectra in Figures 1b and 1c shows that adding AAMIB to OAM largely reduced the P_1^- peak but increased power in the S_1^- and ψ_1^- peaks (see also Table 1).

[29] It is particularly interesting to compare the residuals obtained by removal from the excitation series in Figure 1c of the model expressed by Table 1 (Figure 1d). The reason is that according to *Bizouard et al.* [1998] the atmospheric

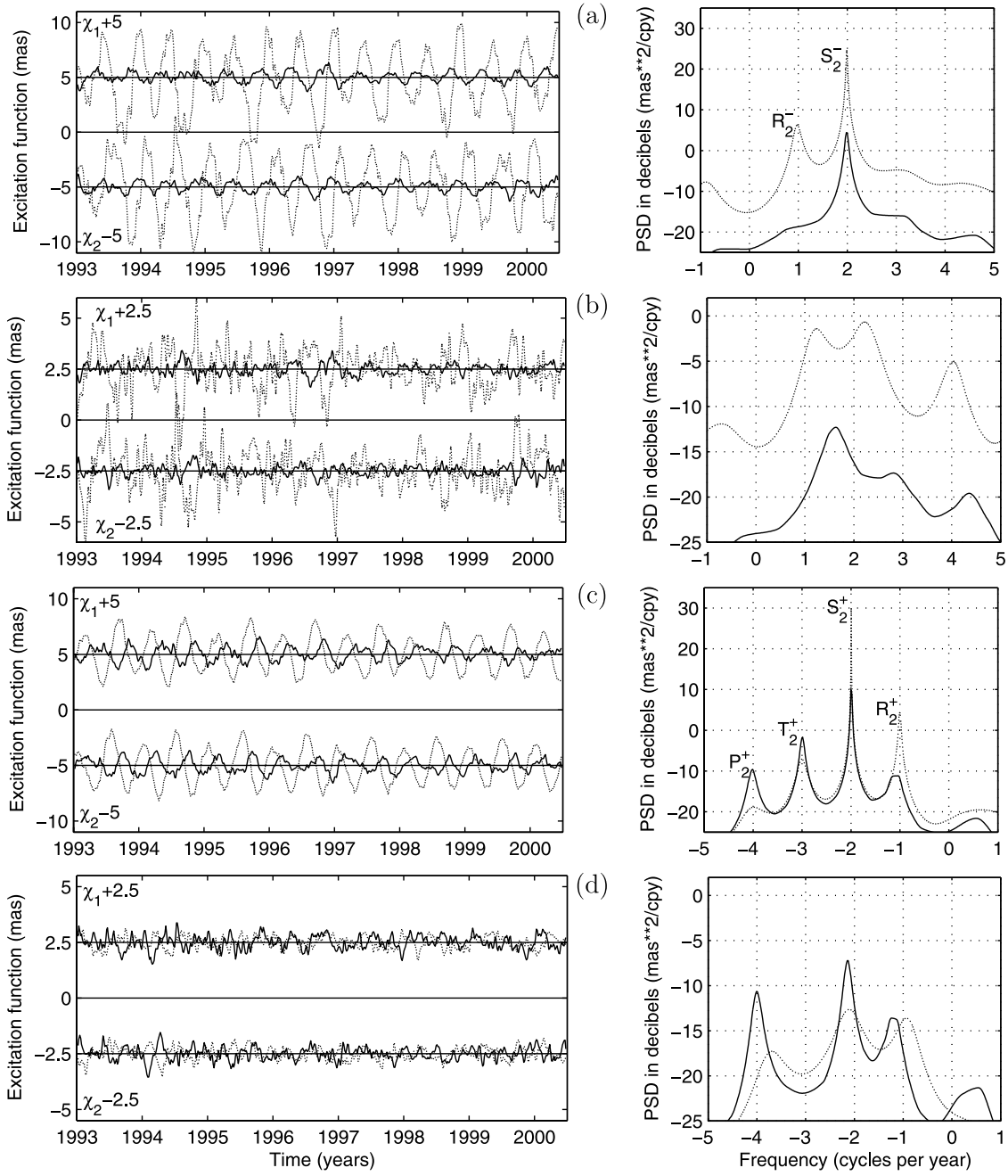

Figure 3. Effective angular momentum functions of the ocean (OAM) demodulated at the frequencies −2 cpsd (Figures 3a and 3b) and +2 cpsd (Figures 3c and 3d). (left) Time domain representation and (right) corresponding maximum entropy power spectra (note that the tidal codes used to identify the spectral peaks refer to the original OAM functions, before demodulation). The following terms of the oceanic excitation are shown: (a, c) the matter term (solid line) and the motion term (dotted line) of OAM; and (b, d) same as in Figures 3a and 3c but after removal from each signal of the model comprising the first-order polynomial and sinusoids with periods ±1, ±1/2, and ±1/3 years (see Table 4 for the parameters of the model).

contribution to nutation is not strictly harmonic but contains also a broadband variability at the level of 0.1 mas. We expect that the dynamic ocean response to the diurnal atmospheric forcing can contribute significantly to this effect. Such irregular component in the differences between the observed and modeled nutation in MHB2000 [*Mathews et al.*, 2002] was also confirmed in a recent study by *Dehant et al.* [2003]. They considered the time variation in the atmospheric (and potentially the oceanic) forcing of nutation as one of the important sources of discrepancies between the theory and observation. The irregular variability of the retrograde diurnal component of the atmospheric and oceanic forcing is a potential source of the observed FCN signal. If such irregular component of nutation is a real physical effect, then it limits the precision of the classical precession-nutation models and indicates the need for

Table 1a. Periodical Components of Atmospheric and Nontidal Oceanic Contributions to Nutation[a]

Term	Excitation		Nutation			
	Amplitude	Phase	Amplitude	Phase	In-Phase	Out-of-Phase
Excitation: ψ_1^- Component; Nutation: Retrograde Annual ($T = -365.26$ days)						
Air pressure	0.196 ± 0.057	79.3 ± 16.7	104.3	−16.4	100.1 ± 37.7	−29.5 ± 37.8
Air pressure IB	0.137 ± 0.036	140.5 ± 15.2	72.9	44.8	51.8 ± 27.2	51.3 ± 27.2
Wind	2.155 ± 0.301	147.5 ± 8.0	11.5	53.2	6.9 ± 2.3	9.2 ± 2.3
Ocean mass	0.233 ± 0.073	−175.7 ± 18.0	124.1	88.6	3.1 ± 39.9	124.0 ± 39.9
Ocean currents	0.181 ± 0.091	−141.0 ± 28.8	1.0	124.7	−0.6 ± 0.7	0.8 ± 0.7
AAM					107.0 ± 37.8	−20.3 ± 37.9
AAMIB					58.7 ± 27.3	60.5 ± 27.3
OAM + AAMIB					61.2 ± 48.3	185.3 ± 48.3
Excitation: S_1^- Component; Nutation: Prograde Annual ($T = 365.26$ days)						
Air pressure	1.775 ± 0.056	171.1 ± 1.8	72.9	84.1	−7.5 ± 2.5	−72.5 ± 2.5
Air pressure IB	1.461 ± 0.037	134.2 ± 1.4	60.0	47.2	−40.8 ± 2.1	−44.0 ± 2.1
Wind	13.548 ± 0.274	−17.4 ± 1.2	27.8	75.2	−7.1 ± 0.7	−26.9 ± 0.7
Ocean mass	1.758 ± 0.084	105.0 ± 2.7	72.2	18.0	−68.6 ± 4.3	−22.3 ± 4.3
Ocean currents	2.173 ± 0.092	46.9 ± 2.4	4.5	139.5	3.4 ± 0.3	−2.9 ± 0.3
AAM					−14.6 ± 2.6	−99.4 ± 2.6
AAMIB					−47.9 ± 2.2	−70.9 ± 2.2
OAM + AAMIB					−113.1 ± 4.8	−96.1 ± 4.8
Excitation: P_1^- Component; Nutation: Prograde Semiannual ($T = 182.62$ days)						
Air pressure	0.212 ± 0.061	73.3 ± 16.4	5.5	−37.2	4.4 ± 2.2	−3.3 ± 2.2
Air pressure IB	0.475 ± 0.027	−91.9 ± 3.2	12.3	157.6	−11.3 ± 0.9	4.7 ± 0.9
Wind	18.342 ± 0.258	−168.3 ± 0.8	39.4	−99.0	−6.2 ± 0.6	−38.9 ± 0.6
Ocean mass	0.640 ± 0.092	118.2 ± 8.3	16.5	7.7	16.4 ± 2.7	2.2 ± 2.7
Ocean currents	0.279 ± 0.073	98.1 ± 15.0	0.6	167.4	−0.6 ± 0.2	0.1 ± 0.2
AAM					−1.8 ± 2.3	−42.2 ± 2.3
AAMIB					−17.5 ± 1.1	−34.2 ± 1.1
OAM + AAMIB					−1.7 ± 2.9	−31.9 ± 2.9

[a]Analysis is done over the period 1993.0 to 2000.5. Phase of excitation is referred to the epoch J2000, and phase of nutation is referred to the standard nutation argument. We apply the same convention for representation of the in-phase and out-of-phase coefficients of the circular nutation terms as *Bizouard et al.* [1998]. Units are degrees for the phase and mas (μas) for the excitation (nutation) amplitudes.

further regular monitoring of the celestial pole offsets. Modeling the corresponding processes in the atmosphere and in the oceans is of crucial importance for future development of the research concerning precession and nutation of the Earth [*Dehant and Brzeziński*, 2004; *Brzeziński*, 2003]. For similar reasons, it is also important to trace the irregular AAM and OAM signals within the prograde diurnal and retrograde/prograde semidiurnal frequency bands.

[30] The comparison of the residuals in the time domain, done in Figure 1d, shows that the dynamic signal is highly coherent with the non-IB excitation. That is confirmed by the corresponding power spectra which show similar shape despite the difference in energy levels. The correlation coefficient between these two series is 0.68, 0.65 for the χ_1, χ_2 components, respectively, and the complex correlation coefficient has a magnitude of 0.68 and argument of only 11°. After integrating the cross power spectrum over the frequency range from −3 to +3 cycles per year, shown in the spectral plots, the complex correlation coefficient did not change its magnitude, but the argument increased to about 20°. The AAMIB signal has much lower variance than the other two (0.36 mas^2 versus 1.28 mas^2 for AAM and 2.56 mas^2 for OAM + AAMIB), but its correlation with the dynamic model is still high (0.53, 0.48 for χ_1, χ_2, respectively). Finally we note that the residual dynamic excitation shows significant excess of power in the vicinity of the FCN frequency in comparison to the IB and non-IB models, which is important for future excitation studies of the observed FCN signal.

Table 1b. Celestial Pole Offset at J2000[a]

Term	Excitation, K_1^- Component		Celestial Pole Offset, Constant	
	χ_1	χ_2	$d\psi \sin \varepsilon_o$	$d\varepsilon$
Air pressure	0.273 ± 0.064	−0.280 ± 0.061	−25.5 ± 11.5	25.4 ± 11.5
Air pressure IB	0.054 ± 0.036	−0.846 ± 0.030	−6.1 ± 3.7	77.9 ± 3.2
Wind	−15.624 ± 0.280	2.657 ± 0.278	−27.3 ± 0.7	4.6 ± 0.6
Ocean mass	−0.006 ± 0.087	0.609 ± 0.087	1.4 ± 8.3	−56.1 ± 8.3
Ocean currents	0.106 ± 0.082	0.171 ± 0.083	0.2 ± 0.3	0.3 ± 0.3
AAM			−52.8 ± 11.5	30.0 ± 11.5
AAMIB			−33.4 ± 3.8	82.5 ± 3.3
OAM + AAMIB			−31.8 ± 9.1	26.7 ± 8.9

[a]Units are mas for the excitation function and μas for the celestial pole coordinates.

Table 2. Contributions to the Prograde Annual Nutation From Individual Effects[a]

	In-Phase	Out-of-Phase
Anelasticity	10	4
Ocean tide load	21	−23
Ocean tide currents	0	1
CMB electromagnetic coupling	0	−3
ICB electromagnetic coupling	14	−3
Geodesic nutation	30.4	0
Sun-synchronous	10.4	−108.2

[a]After *Mathews et al.* [2002, Tables 5 and 7]. CMB is the core-mantle boundary, and ICB is the inner core boundary. Units are μas.

[31] *Bizouard et al.* [1998] discovered time variability of the atmospheric contribution to the nutation amplitudes, that is the effect which is included in the AAM signals depicted in Figure 1d. *Bizouard et al.* [1998, p. 561] concluded that this variability "yields a considerably better agreement with the VLBI nutation data when using the AAM function without the IB correction for ocean response, which indicates that this correction is not adequate for nearly diurnal variations." Here we obtained an independent strong confirmation that the non-IB model, that is, the rigid ocean response, yields in the nutation band quite good approximation for the dynamic model. Note, however, that this is only valid for the irregular variation but not for the Sun-fixed S_1^- term of the excitation which is represented in Figure 1c and Table 1 by the prograde annual harmonic.

[32] Let us consider now the regular part of the atmospheric and oceanic contributions to nutation, shown in Table 1. In Table 1 we disregard the estimated drifts expressed by the time derivatives of the nutation angles, contributing to precession, mostly due to the fact that the oceanic influences are not significant in view of their formal errors. In case of the constant offset, the oceanic influence coming almost entirely from the matter term is similar in size to the atmospheric effect. The total offset is in the same direction as that estimated previously from the atmospheric data alone but almost 3 times smaller. In case of the P_1^- term corresponding to the prograde semiannual nutation, the dominant contribution is from the wind term of AAM. The ocean current term has a negligible influence while OAM and AAMIB matter terms tend to cancel each other, as we already concluded from the spectral plots shown in Figures 1b and 1c. In case of the ψ_1^- term and the corresponding retrograde annual nutation, the estimated atmospheric and oceanic contributions are relatively large but so are their formal errors. This can be explained by the fact that quite weak waves in the excitation function are strongly amplified due to the vicinity of the FCN resonance.

[33] We will consider now in more detail the S_1^- term of excitation which contributes to the prograde annual nutation. This Sun-fixed thermal tide is the largest term of all AAM and OAM series and therefore could be quite accurately determined from our analysis. More importantly, other known contributions to the prograde annual nutation are considerably smaller than these considered here, therefore we can perform the excitation balance and compare to the VLBI observations. This nutation term was treated at length in the recently adopted theory of nutation MHB2000 [*Mathews et al.*, 2002]. In addition to the direct effect of the tidal gravitation, there are several contributions which had to be taken into account. After changing to our phase convention, these contributions are shown in Table 2. The "Sun-synchronous" component is the empirical value which was introduced in order to reach the best agreement with the VLBI observations. This value expresses both the atmospheric and the nontidal oceanic influences which have not been modeled in MHB2000. In addition, it can be influenced by other Sun-synchronous effects (having 24 hours periodicity), such as solar heating of VLBI antennas [*Mathews et al.*, 2002, section 2.6].

[34] Our estimates of the out-of-phase amplitude are similar for all three models and in quite good agreement with the VLBI observations. In case of the in-phase component, there is a large discrepancy between results from different models and from the VLBI observations. The best overall fit to the VLBI data is from the non-IB model. The dynamic model yields good agreement with observation for the out-of-phase component but the worst fit for the in-phase one. That may be in part due to the inaccuracies in the representation of the S_1 barometric tide in the models, mentioned in section 3. Another possible source of discrepancy is an artificial S_1 harmonic caused by the solar heating of the VLBI antennas; see *IERS* [2003, chapter 7] for description of this effect.

4.2. Excitation of Prograde Diurnal Polar Motion

[35] The prograde diurnal component of the atmospheric and oceanic excitation of polar motion, shown in Figure 2 and Table 3, differs in several aspects from the retrograde diurnal component discussed in section 4.1. First, there is no more discrepancy in size between the motion terms of the AAM and OAM series, though there is a large difference in phase (Figure 2a and Table 3). Second, the residual signals of the matter term shown in Figure 2d contain considerably less power than their retrograde counterparts depicted in Figure 1d. The variances are 0.21 mas^2 for AAMIB, 0.68 mas^2 for AAM, and 0.99 mas^2 for OAM + AAMIB. Given the low value of the transfer function, the corresponding irregular variation in polar motion is very weak (<1 μas). Third, the spectral structure of all excitation signal plotted in Figures 2a and 2c is simpler. It consists of the dominant S_1^+ peak and only two side lobes of similar size expressing the annual modulation of the S_1 tide, the P_1^+ and K_1^+ harmonics. That can be seen from Table 3, while in the spectral plots shown in Figures 2a to 2c the K_1^+ peak does not appear because, as already mentioned, our program of spectral estimation removes mean value from the input series.

[36] In case of the matter term the AAM and AAMIB signals are quite similar while both the OAM term (Figure 2b) and the sum OAM + AAMIB (Figure 2c) have larger amplitudes (up to factor of 2) and are significantly delayed in phase. We may conclude that the OAM + AAMIB model yields considerably different results in the prograde diurnal band than the IB and non-IB models. Also, when comparing in more detail the irregular residual signals, depicted in Figure 2d, no significant correlation was found between OAM + AAMIB and either AAM or AAMIB.

[37] Let us now consider the regular part of the atmospheric and oceanic contribution to prograde diurnal polar motion, expressed by the model with parameters shown in Table 3. In case of the P_1^+ and K_1^+ harmonics, various

Table 3. Atmospheric and Nontidal Oceanic Contributions to Prograde Diurnal Polar Motion[a]

Term	Excitation		Polar Motion[b]			
	Amplitude	Phase	Amplitude	Phase	$p_x^{\sin}$	$p_x^{\cos}$
			P_1^+ Component, Period 1.0027454 day			
Wind	0.224 ± 0.053	39.5 ± 13.5	0.5	60.6	−0.5 ± 0.2	0.3 ± 0.2
Air pressure	0.324 ± 0.040	−8.1 ± 7.1	0.8	13.0	−0.2 ± 0.1	0.8 ± 0.1
Air pressure IB	0.340 ± 0.028	−43.5 ± 4.7	0.8	−22.4	0.3 ± 0.1	0.8 ± 0.1
Ocean mass	0.715 ± 0.093	121.9 ± 7.4	1.7	143.0	−1.0 ± 0.3	−1.4 ± 0.3
Ocean currents	0.568 ± 0.073	−97.7 ± 7.4	1.3	−76.6	1.3 ± 0.2	0.3 ± 0.2
AAM					−0.7 ± 0.2	1.1 ± 0.2
AAMIB					−0.2 ± 0.2	1.1 ± 0.2
OAM + AAMIB					0.1 ± 0.4	0.0 ± 0.4
Triaxiality					−4.8	2.7
Ocean tide					26.1	51.2
			S_1^+ Component, Period 0.9999999 day			
Wind	2.243 ± 0.038	90.8 ± 1.0	5.2	−91.5	5.2 ± 0.1	−0.1 ± 0.1
Air pressure	2.030 ± 0.042	12.6 ± 1.2	4.9	−169.7	0.9 ± 0.1	−4.8 ± 0.1
Air pressure IB	1.583 ± 0.023	−8.9 ± 0.8	3.8	168.8	−0.7 ± 0.1	−3.8 ± 0.1
Ocean mass	3.281 ± 0.089	66.5 ± 1.6	7.9	−115.8	7.2 ± 0.3	−3.5 ± 0.3
Ocean currents	2.256 ± 0.091	−137.7 ± 2.3	5.2	40.0	−3.4 ± 0.3	4.0 ± 0.3
AAM					6.1 ± 0.1	−4.9 ± 0.1
AAMIB					4.5 ± 0.1	−3.9 ± 0.1
OAM + AAMIB					8.3 ± 0.4	−3.4 ± 0.4
Triaxiality					0.0	0.0
Ocean tide					−0.6	−1.2
			K_1^+ Component, Period 0.9972696 day			
Wind	0.196 ± 0.061	70.1 ± 18.2	0.5	−109.7	0.4 ± 0.2	−0.2 ± 0.2
Air pressure	0.390 ± 0.064	−48.0 ± 9.3	0.9	132.1	−0.7 ± 0.2	−0.6 ± 0.2
Air pressure IB	0.208 ± 0.034	−70.0 ± 8.5	0.5	110.2	−0.5 ± 0.1	−0.2 ± 0.1
Ocean mass	0.632 ± 0.120	143.8 ± 10.9	1.5	−36.0	0.9 ± 0.4	1.2 ± 0.4
Ocean currents	0.419 ± 0.104	−72.8 ± 14.0	1.0	107.4	−0.9 ± 0.3	−0.3 ± 0.3
AAM					−0.3 ± 0.2	−0.8 ± 0.2
AAMIB					−0.1 ± 0.2	−0.4 ± 0.2
OAM + AAMIB					−0.1 ± 0.5	0.5 ± 0.5
Triaxiality					14.3	−8.2
Ocean tide					−77.5	−151.7

[a]Analysis is done over the period 1993.0 to 2000.5. Phase of the excitation is referred to the epoch J2000, and phase of polar motion is referred to the standard astronomical argument. For comparison, contributions from the ocean tide and due to the torque of the tidal gravitation on the triaxiality of the Earth are shown also, taken from [*IERS*, 2003, Tables 8.2a and 5.1]. We apply the same convention of the development as *IERS* [2003]; see footnote b for a brief description. Units are degrees for the phase and mas (μas) for the excitation (polar motion) amplitudes.

[b]The x and y components of polar motion $p = p_x - ip_y$ are expressed as $p_x = p_x^{\sin}\sin(\arg) + p_x^{\cos}\cos(\arg)$, $p_y = p_y^{\sin}\sin(\arg) + p_y^{\cos}\cos(\arg)$, with $\arg = (\mathrm{GMST} + \pi) + k_1 l_m + k_2 l_s + k_3 F + k_4 D + k_5 \hat{\Omega}$, where l_m, l_s, F, D, and $\hat{\Omega}$ are the fundamental arguments used in the nutation theory, GMST denotes Greenwich mean sidereal time, and $k_1, \ldots, k_5$ are integer coefficients. Only $p_x^{\sin}$ and $p_x^{\cos}$ are shown because for the prograde harmonics, $p_y^{\sin} = -p_x^{\cos}$, $p_y^{\cos} = p_x^{\sin}$.

contributions cancel each other and the total amplitude corresponding to the dynamic model is practically zero. Hence the only significant contribution is from the S_1^+ term which is represented in the demodulated series by the retrograde annual sinusoid. The dynamic model yields a total amplitude in polar motion of 9 μas, slightly larger than the non-IB and IB models (8 and 6 μas, respectively) and with phase delay of 17° and 19°, respectively. As the ocean tide contribution is about 7 times smaller [*IERS*, 2003, Table 8.2a], there is a good chance that future subdiurnal determinations of polar motion will verify our estimate of the nontidal effect.

4.3. Excitation of Semidiurnal Polar Motion

[38] With the 6-hourly sampling of the AAM series it is not possible to resolve the retrograde and prograde components of the semidiurnal band; see Appendix B of *Brzeziński et al.* [2002] for extensive discussion. If we perform the complex demodulation of AAM at frequencies -2Ω, $+2\Omega$ and then compute the power spectra, the prograde spectrum will be the mirror reflection of the retrograde one with respect to the frequency 2 cycles/d, which is the frequency of the S_2 tide and at the same time is the Nyquist frequency for the input AAM series. Each peak of the spectrum will express the aggregate power of two oscillations with frequencies 2 cycles/d ± k cycles/yr. Hence the S_2 peak ($k = 0$) will express the sum of the S_2^- and S_2^+ amplitudes, the R_2 peak ($k = 1$) will express the sum of the T_2^- and R_2^+ amplitudes, etc. There is no such problem with the OAM data which are sampled hourly, though the reliability of the estimates should be treated with caution, as discussed in section 3. Because of the reasons explained above, in this section we will show the results concerning the oceanic excitation at semidiurnal frequencies. The only estimate of the atmospheric excitation will be that given in Table 4 for the S_2 term, under additional assumption that the motion is prograde.

[39] From Figure 3 it can be seen that there is a significant asymmetry between the retrograde and prograde components of the semidiurnal oceanic excitation. Much larger, but at the same time also much noisier is the retrograde component with dominant contribution from the motion term. In case of the prograde component, the motion term is still larger than the matter term, but its behavior is rather

Table 4. Atmospheric and Nontidal Oceanic Contributions to Semidiurnal Polar Motion[a]

Term	Polar Motion[b] $p_x^{\sin}$	$p_x^{\cos}$	$p_y^{\sin}$	$p_y^{\cos}$
S_2Component,[c] *Period 0.5000000 day*				
Wind	−2.6 ± 0.2	1.6 ± 0.2	−1.6 ± 0.2	−2.6 ± 0.2
Air pressure	−1.9 ± 0.1	0.0 ± 0.1	0.0 ± 0.1	−1.9 ± 0.1
Air pressure IB	−1.1 ± 0.1	0.2 ± 0.1	−0.2 ± 0.1	−1.1 ± 0.1
Ocean mass	0.0 ± 0.1	−0.2 ± 0.1	0.0 ± 0.1	−1.6 ± 0.1
Ocean currents	0.4 ± 0.1	6.4 ± 0.1	1.6 ± 0.1	1.0 ± 0.1
Ocean nontidal total	0.4 ± 0.1	6.2 ± 0.1	1.6 ± 0.1	−0.6 ± 0.1
Ocean tide	−144.1	63.6	59.2	86.6
R_2Component,[d] *Period 0.4993165 day*				
Ocean mass	0.0 ± 0.1	0.1 ± 0.1	−0.1 ± 0.1	0.0 ± 0.1
Ocean currents	−1.3 ± 0.1	−0.7 ± 0.1	0.1 ± 0.1	0.7 ± 0.1
Ocean nontidal total	−1.3 ± 0.1	−0.6 ± 0.1	0.0 ± 0.1	0.7 ± 0.1
Ocean tide	1.2	−0.6	−0.5	−0.7

[a]Analysis is done over the period 1993.0 to 2000.5. Only the components for which the OAM contribution exceeds the level of 1 μas are included. For comparison, contributions from the ocean tide taken from *IERS* [2003, Table 8.2b] are shown also. Unit is μas for the polar motion coefficients.

[b]Polar motion is expressed in the same way as it was defined in the footnote of Table 3. We merged each pair of the prograde and retrograde semidiurnal components with the same period into a single term expressing elliptical motion, which made it necessary to show the sine and cosine coefficients for both the x and y coordinates of the pole.

[c]The S2 component of AAM is a sum of prograde and retrograde contributions $\chi = A^+ \exp(i\,\arg) + A^- \exp(-i\,\arg)$, with $\arg = 2(\mathrm{GMST} + \pi) - 2F + 2D - 2\Omega$, where A^+, A^- are complex amplitudes. The corresponding polar motion equals approximately $p = 0.001\,[A^+ \exp(i\,\arg) - A^- \exp(-i\,\arg)]$. From the 6-hourly estimates of AAM it is only possible to determine the sum of A^+ and A^-; see *Brzeziński et al.* [2002, Appendix B] for detailed discussion of this issue. The coefficients of the atmospheric contribution to the S_2 component of polar motion were computed under assumption that the motion is prograde ($A^- = 0$). However, it can be seen that when trying various combinations of A^+ and A^- while keeping their sum constant, one can derive quite different values of the corresponding coefficients of polar motion.

[d]Atmospheric contributions are not given for R_2 because with the 6-hourly sampling it is not possible to resolve the R_2 and T_2 harmonics (see *Brzeziński et al.* [2002] for details).

regular and can be greatly reduced by subtracting the harmonic model.

[40] The dominant component of the regular part shown in Table 4 is the S_2 term. The main contribution is from the ocean currents and the total amplitude of polar motion is about 6 μas. The motion of the pole is elliptical with most variability along the x axis of the Earth-fixed reference system. When adding the estimated atmospheric contribution, the amplitude increases to ∼9 μas, similar to that of the prograde diurnal polar motion. However, in contrast to the S_1^+ term, the contribution of the gravitational ocean tide is significant. In fact, the total effect as given by *IERS* [2003, Table 8.2a] is almost 20 times larger than the nontidal part estimated here. For the R_2 term both the tidal and nontidal oceanic contributions to polar motion only slightly exceed the level of 1 μas and are hence very small.

5. Summary and Conclusions

[41] We used in this study a new 7.5-year time series of nontidal OAM, computed from a near-global barotropic model [*Ponte and Ali*, 2002], to estimate the influence of the atmospherically driven ocean dynamics on nutation and on diurnal and semidiurnal polar motions. The OAM series is sampled hourly to resolve the diurnal and semidiurnal spectral bands. However, the ocean model is driven by 6-hourly surface wind and pressure fields linearly interpolated to the model time step of 1 min. Thus the forcing does not resolve the full nature of the S_2 barometric tide, and the linear interpolation can significantly distort the representation of the S_1 barometric tide. For this reason the results reported here should be treated with caution.

[42] Such an excitation study should account in a consistent way for the atmospheric influence on Earth rotation. We used AAM series calculated from the NCEP-NCAR reanalysis wind and surface pressure fields, the same fields used to drive the ocean model. The AAM series contains the non-IB (AAM) and IB (AAMIB) versions of the matter term and are available at 6-hour intervals, which makes it impossible to resolve well the semidiurnal frequency band. A primary purpose of this work was comparison of the excitation functions representing the coupled atmosphere-ocean system corresponding to various models of the ocean response to the atmospheric forcing: (1) the non-IB model, which assumes the rigid ocean, with the aggregated excitation expressed just by AAM; (2) the IB model with the excitation expressed by AAMIB series; and (3) the dynamic model with the excitation expressed by the sum AAMIB + OAM.

[43] By applying the complex demodulation procedure we extracted from the OAM and AAM series the components expressing excitation for retrograde and prograde diurnal and semidiurnal bands. The most important part of analysis concerns the retrograde diurnal component of excitation which perturbs nutation. The reason is that due to the enhancement by the FCN resonance, the corresponding contribution to nutation exceeds the peak-to-peak size of 0.3 mas which is well above the accuracy level of the VLBI measurements of the nutation parameters. A general observation is that in contrast to AAM, the influence of the OAM motion term on nutation is very small. We found nonnegligible oceanic contributions to the constant offset of the celestial pole ($\delta\psi\sin\varepsilon_o = -32$ μas, $\delta\varepsilon = 27$ μas) and to the following components of nutation: retrograde annual (195 μas), prograde annual (148 μas) and prograde semiannual (32 μas); amplitudes given are aggregated contributions from AAMIB + OAM model. In practice, the only contribution to nutation that can be compared to the VLBI determinations is the prograde annual component driven by the Sun-synchronous S_1^- term of the excitation function. Unfortunately, when taking into account the excitation budget of this nutation constituent calculated by *Mathews et al.* [2002], the dynamic model yields worse agreement with observation than the non-IB model.

[44] There are many possible reasons for the noted discrepancies in the prograde annual nutation budget. On the ocean side, apart from possible errors in the simulation of S_1 induced by the linear interpolation of 6-hourly forcing fields, as already noted, the amplitudes of the S_1 barometric fields in NCEP-NCAR are likely an overestimate and phase problems have also been noted [*Ray and Ponte*, 2003]. One can replace linear interpolation scheme with more adequate methods [e.g., *Ponte and Ray*, 2002] and such improvements should increase the reliability of the OAM estimates at diurnal as well as semidiurnal periods. Besides errors in

forcing fields, model physics, domain representation, and other factors can be improved. Comparisons of the present results with those of *Petrov et al.* [1998] indicate that results are quite sensitive to the parameterization of friction in the models. The significantly higher dissipation rates in the model used here lead to more realistic amplitudes for the simulated diurnal variability and account for the much better agreement with the VLBI data for the out-of-phase amplitude of the prograde annual nutation, when compared to the results of *Petrov et al.* [1998]. In this regard, nutation data provides a useful check on the realism of diurnal signals in the models. Better simulations of S_1 in the future will likely include improvements in both the hydrodynamic models and their atmospheric forcing fields, as well as the use of data constraints from altimeter and tide gauge sea level observations.

[45] Uncertainties in all the components of the prograde annual nutation budget are also likely. Direct estimates of tidal oceanic excitation have not been published. Results of *Mathews et al.* [2002] are derived from admittance arguments based on a linear fit of four diurnal tidal lines and can probably be improved. We note that the forcing of S_1^- term is mostly nontidal (i.e., atmospherically forced) in origin, yet tidal effects quoted in section 4.1 are not small compared to the nontidal effects calculated here. We have mentioned problems with NCEP-NCAR representations of the barometric S_1 tide, which could lead to erroneous values of AAM, particularly in the matter terms. Wind terms are probably even less well determined. Further study is thus clearly required to model the S_1 term in the excitation of nutation and polar motion with improved accuracy and to better understand the respective budgets.

[46] After removing from the OAM and AAM series the model comprising the linear trend and the harmonic contributions mentioned above, we considered separately the irregular residual variability. This component is important as a possible source of excitation of the observed FCN signal with variable amplitude between 0.1 and 0.3 mas. Our analysis revealed that the dynamical model shows a significant excess of power in the vicinity of the FCN spectral line, in comparison to the non-IB and IB models. However, even after neglecting the FCN, the remaining variability excite perturbations in nutation at the level of 0.1 mas, hence still an observable effect. The irregular term of OAM + AAMIB is significantly correlated with the non-IB AAM counterpart: the complex correlation coefficient has a magnitude of almost 70% and an argument between 10° and 20°. These results are consistent with the finding of *Bizouard et al.* [1998] that the non-IB AAM contribution to nutation is significantly correlated with the irregular variation of the celestial pole offsets monitored by VLBI. Thus, in contrast with excitation studies at long periods, non-IB matter terms are preferable when comparing VLBI nutation measurements with AAM data.

[47] In case of the prograde diurnal component, the matter terms for AAM and AAMIB models are quite similar while that derived from the dynamic model (OAM + AAMIB) has significantly larger amplitude, up to factor of 2, and is delayed in phase by about 17°. The only nonnegligible contribution to polar motion found was that related to the S_1^+ harmonic. The dynamic model gives 9 μas for the total amplitude of the S_1^+ term in polar motion. This amplitude is rather small, but as the ocean tide contribution is ∼7 times smaller, there is a good chance that future subdiurnal determinations of polar motion will verify our estimate.

[48] When considering the semidiurnal excitation, we found that the largest contribution to polar motion from the dynamically coupled atmosphere-ocean system is an elliptical S_2 component with major semiaxis of ∼9 μas. However, even if we neglect the problem of reliability of OAM estimates associated with the 6-hourly forcing of the ocean model, it would be difficult to verify this estimate from the observations of polar motion. The reason is that the ocean tide contribution to the S_2 component is about 20 times larger than the nontidal effect, and it is likely that the uncertainty of the ocean tide model is comparable to the much smaller nontidal oceanic and atmospheric effects.

[49] **Note added in proof.** Since this paper was submitted, a study addressing similar topics [*de Viron et al.*, 2004] has appeared in the literature. Besides other geodetic parameters, de Viron et al. estimate the nontidal oceanic effect on nutation using an ocean modeling approach very different from the one we used here.

[50] **Acknowledgment.** This work has been supported by the Polish Ministry of Scientific Research and Information Technology under grant 5 T12E 039 24. R.P. was supported by NASA under contract 1206432 with the Jet Propulsion Laboratory.

References

Barnes, R. T. H., R. Hide, A. A. White, and C. A. Wilson (1983), Atmospheric angular momentum fluctuations, length-of-day changes and polar motion, *Proc. R. Soc. London, Ser. A*, *387*, 31–73.

Bingham, C., M. D. Godfrey, and J. W. Tukey (1967), Modern techniques of power spectrum estimation, *IEEE Trans. Audio Electroacoust.*, *AU-15*, 56–66. (Reprinted in *Modern Spectrum Analysis*, edited by D. G. Childers, pp. 6–16, IEEE Press, New York, 1978.)

Bizouard, C., A. Brzeziński, and S. D. Petrov (1998), Diurnal atmospheric forcing and temporal variations of the nutation amplitudes, *J. Geod.*, *72*, 561–577.

Brzeziński, A. (1994a), Polar motion excitation by variations of the effective angular momentum function, II: Extended model, *Manuscr. Geod.*, *19*, 157–171.

Brzeziński, A. (1994b), Diurnal and semidiurnal polar motions estimated from the intensive atmospheric angular momentum data, *Ann. Geophys., Part I*, *12*, Suppl. I, C177.

Brzeziński, A. (1995), On the interpretation of maximum entropy power spectrum and cross-power spectrum in earth rotation investigations, *Manuscr. Geod.*, *20*, 248–264.

Brzeziński, A. (2000), The CEP and geophysical interpretation of modern Earth rotation observations, in *Proceedings of the IAU Colloquium 178 "Polar Motion: Historical and Scientific Problems," Conf. Ser.*, vol. 208, edited by S. Dick, D. McCarthy, and B. Luzum, pp. 585–594, Astron. Soc. of the Pac., San Francisco, Calif.

Brzeziński, A. (2003), Oceanic excitation of polar motion and nutation - an overview, in *Proceedings of the IERS Workshop on Combination Research and Global Geophysical Fluids*, edited by B. Richter, W. Schwegmann, and W. R. Dick, *IERS Tech. Note*, *30*, 144–149.

Brzeziński, A., and N. Capitaine (1993), The use of the precise observations of the celestial ephemeris pole in the analysis of geophysical excitation of Earth rotation, *J. Geophys. Res.*, *98*(B4), 6667–6675.

Brzeziński, A., C. Bizouard, and S. D. Petrov (2002), Influence of the atmosphere on Earth rotation: What new can be learned from the recent atmospheric angular momentum estimates?, *Surv. Geophys.*, *23*, 33–69.

Dehant, V., and A. Brzeziński (2004), Working Group on Nutation, in *Proceedings of the XXV IAU General Assembly*, edited by O. Engvold, *Trans. Int. Astron. Union, XXVB*, in press.

Dehant, V., C. Bizouard, J. Hinderer, H. Legros, and M. Greff-Lefftz (1996), On atmospheric pressure perturbations on precession and nutations, *Phys. Earth Planet. Inter.*, *96*, 25–39.

Dehant, V., M. Feissel-Vernier, O. de Viron, C. Ma, M. Yseboodt, and C. Bizouard (2003), Remaining error sources in the nutation at the sub-

milliarcsecond level, *J. Geophys. Res.*, *108*(B5), 2275, doi:10.1029/2002JB001763.

de Viron, O., J. P. Boy, and H. Goosse (2004), Geodetic effects of the ocean response to atmospheric forcing in an ocean general circulation model, *J. Geophys. Res.*, *109*, B03411, doi:10.1029/2003JB002837.

Dickman, S. R. (1988), Theoretical investigation of the oceanic inverted barometer response, *J. Geophys. Res.*, *93*(B12), 14,941–14,946.

Dickman, S. R. (1998), Determination of oceanic dynamic barometer corrections to atmospheric excitation of Earth rotation, *J. Geophys. Res.*, *103*(B7), 15,127–15,143.

Eubanks, T. M. (1993), Variations in the orientation of the Earth, in *Contributions of Space Geodesy to Geodynamics: Earth Dynamics*, *Geodyn. Ser.*, vol. 24, edited by D. E. Smith and D. L. Turcotte, pp. 1–54, AGU, Washington, D. C.

Mathews, P. M., T. A. Herring, and B. A. Buffett (2002), Modeling of nutation and precession: New nutation series for nonrigid Earth and insights into the Earth's interior, *J. Geophys. Res.*, *107*(B4), 2068, doi:10.1029/2001JB000390.

International Earth Rotation Service (2003), IERS conventions 2003, edited by D. McCarthy and G. Petit, *IERS Tech. Note*, *32*, Paris. (Available at http://maia.usno.navy.mil/conv2003.html).

Kalnay, E., et al. (1996), The NMC/NCAR 40-year reanalysis project, *Bull. Am. Meteorol. Soc.*, *77*(3), 437–471.

Nastula, J., and R. M. Ponte (1999), Further evidence for oceanic excitation of polar motion, *Geophys. J. Int.*, *139*, 123–130.

Petrov, S. D. (1998), Modeling geophysical excitation of Earth rotation: Stochastic and nonlinear approaches, Ph.D. thesis, Space Res. Cent. of the Pol. Acad. of Sci., Warsaw.

Petrov, S. D., A. Brzeziński, and J. Nastula (1998), First estimation of the non-tidal oceanic effect on nutation, in *Proceedings of the Journées Systèmes de Référence Spatio-Temporels 1998*, edited by N. Capitaine, pp. 136–141, Paris Obs., Paris.

Ponte, R. M. (1993), Variability in a homogeneous global ocean forced by barometric pressure, *Dyn. Atmos. Oceans*, *18*, 209–234.

Ponte, R. M. (1997), Oceanic excitation of daily to seasonal signals in Earth rotation: Results from a constant-density numerical model, *Geophys. J. Int.*, *130*, 469–474.

Ponte, R. M., and A. H. Ali (2002), Rapid ocean signals in polar motion and length of day, *Geophys. Res. Lett.*, *29*(15), 1711, doi:10.1029/2002GL015312.

Ponte, R. M., and R. D. Ray (2002), Atmospheric pressure corrections in geodesy and oceanography: A strategy for handling air tides, *Geophys. Res. Lett.*, *29*(24), 2153, doi:10.1029/2002GL016340.

Ray, R. D., and R. M. Ponte (2003), Barometric tides from ECMWF operational analyses, *Ann. Geophys.*, *21*, 1897–1910.

Salstein, D. A., D. M. Kann, A. J. Miller, and R. D. Rosen (1993), The subbureau for atmospheric angular momentum of the International Earth Rotation Service: A meteorological data center with geodetic applications, *Bull. Am. Meteorol. Soc.*, *74*, 67–80.

Sasao, T., and J. M. Wahr (1981), An excitation mechanism for the free 'core nutation', *Geophys. J. R. Astron. Soc.*, *64*, 729–746.

A. H. Ali, Raytheon ITSS, 299 N. Euclid Ave., Suite 500, Pasadena, CA 91101, USA. (aali@pacific.jpl.nasa.gov)

A. Brzeziński(corresponding author), Space Research Centre, Polish Academy of Sciences, Bartycka 18A, 00-716 Warsaw, Poland. (alek@cbk.waw.pl)

R. M. Ponte, Atmospheric and Environmental Research, Inc., 131 Hartwell Avenue, Lexington, MA 02421-3126, USA. (rponte@aer.com)

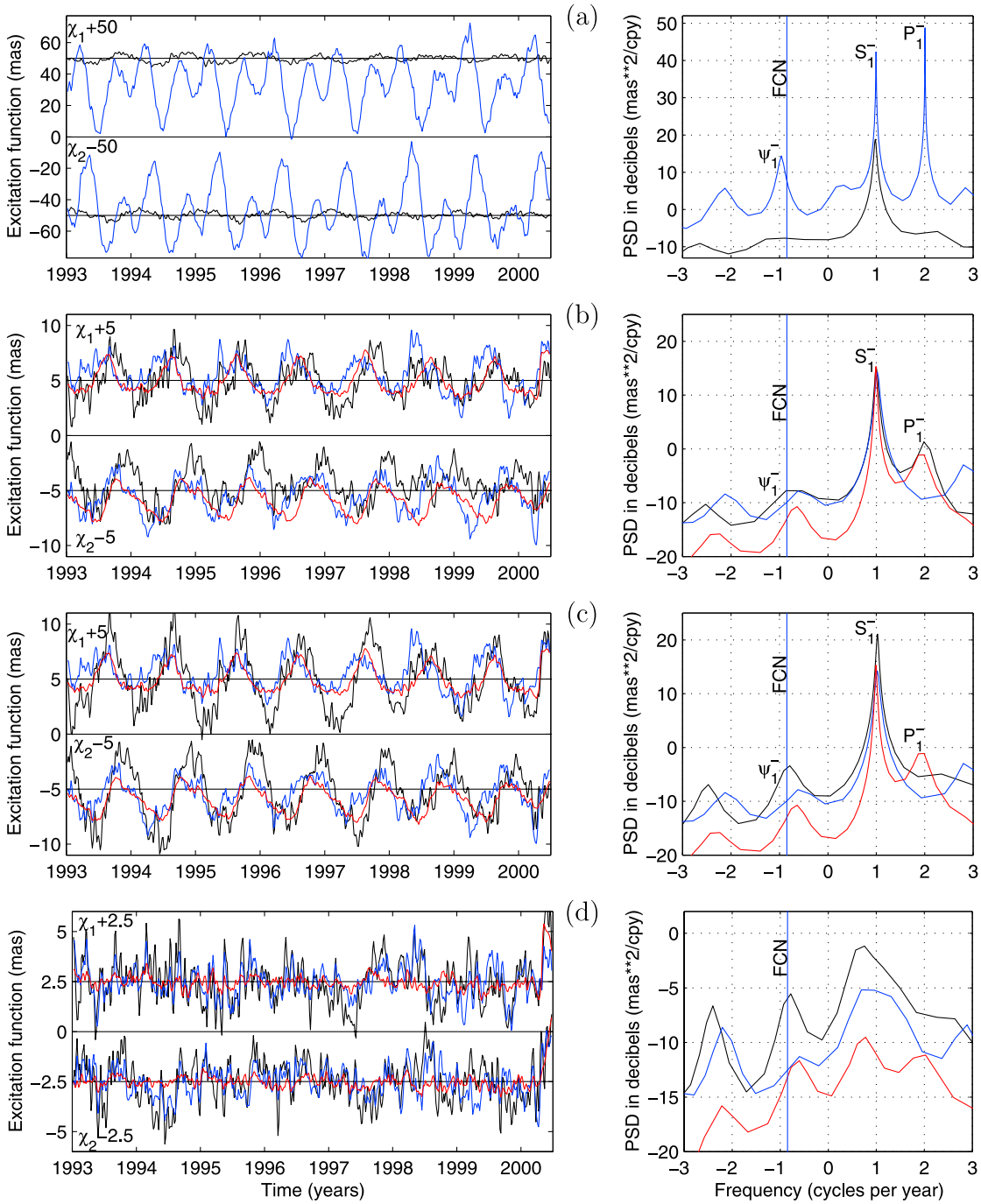

Figure 1. Celestial effective angular momentum (CEAM) functions, that is, the EAM functions demodulated at the frequency −1 cpsd, of the atmosphere and of the ocean. (left) Time domain representation of CEAM and (right) maximum entropy estimate of the corresponding power spectral density (PSD) function (note that the tidal codes used to identify the spectral peaks refer to the original EAM functions). The following terms of the excitation are shown: (a) the motion terms of AAM (blue) and OAM (black); (b) the matter terms of AAM (blue), AAMIB (red), and OAM (black); (c) the matter terms of the system atmosphere/ocean for different models of the ocean response to atmospheric forcing: AAM (blue), AAMIB (red) and AAMIB + OAM (black); see text for additional discussion; and (d) same as in Figure 1c but after removal from each signal of the model comprising the first-order polynomial and sinusoids with periods ±1, ±1/2, and ±1/3 years (see Table 1 for the parameters of the model).

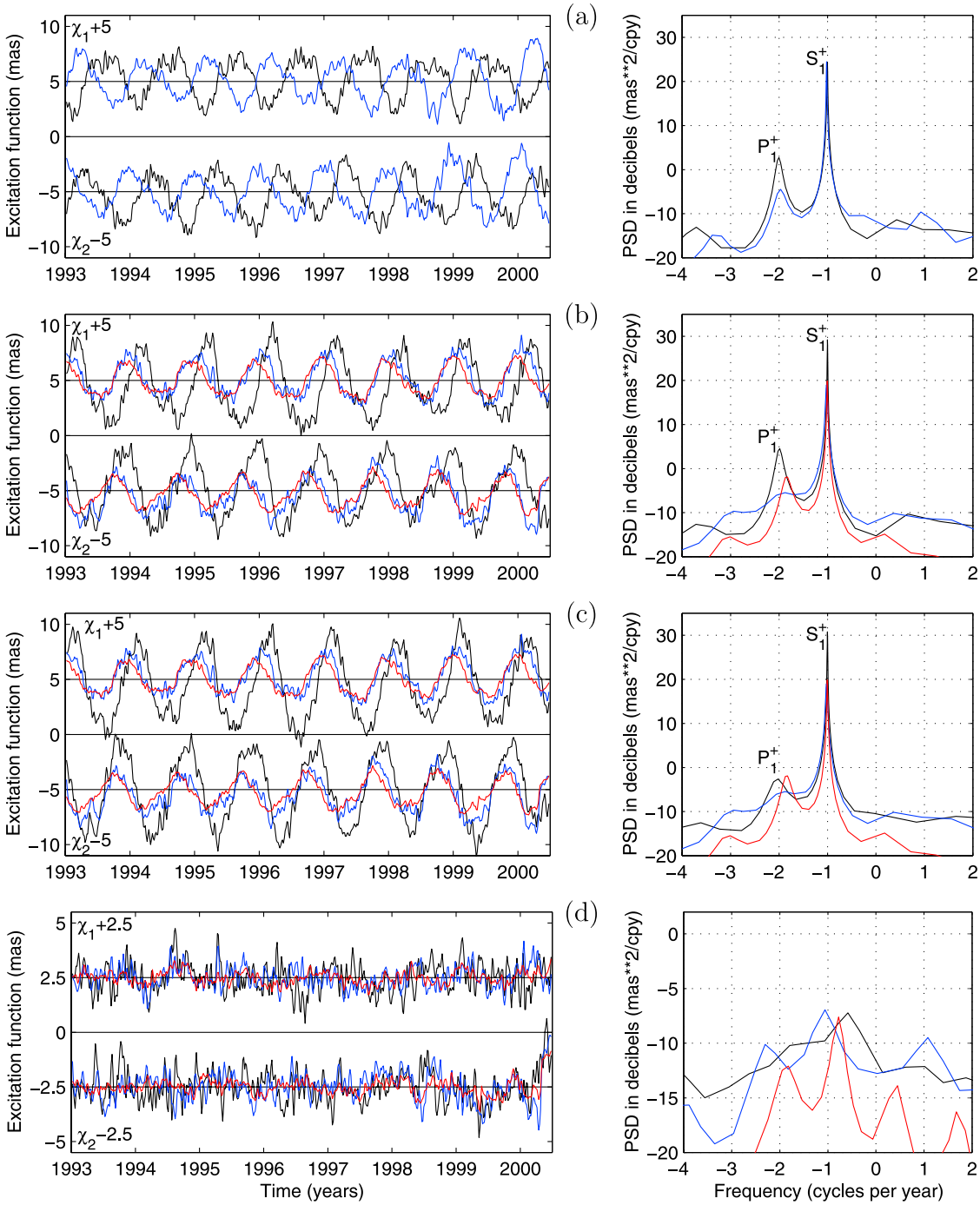

Figure 2. Effective angular momentum (EAM) functions of the atmosphere and of the ocean, demodulated at frequency +1 cpsd. (left) Time domain representation and (right) corresponding maximum entropy power spectra (note that the tidal codes used to identify the spectral peaks refer to the original EAM functions, before demodulation). The following terms of the excitation are shown: (a) the motion terms of AAM (blue) and OAM (black); (b) the matter terms of AAM (blue), AAMIB (red), and OAM (black); (c) the matter terms of the system atmosphere/ocean for different models of the ocean response to atmospheric forcing: AAM (blue), AAMIB (red) and AAMIB + OAM (black); see text for additional discussion; and (d) same as in Figure 2c but after removal from each signal of the model comprising the first-order polynomial and sinusoids with periods ±1, ±1/2, ±1/3 years (see Table 3 for the parameters of the model).